Available online at www.sciencedirect.com
ScienceDirect
Trans. Nonferrous Met. Soc. China 21(2011) s328−s332
Transactions of Nonferrous Metals Society of China
www.tnmsc.cn

Microstructure and nanohardness of Ti−48%Al alloy prepared by rapid solidification under different cooling rates

WANG Hong-wei[1, 2], ZHU Dong-dong[1], ZOU Chun-ming[1], WEI Zun-jie[1]

1. School of Materials Science and Engineering, Harbin Institute of Technology, Harbin 150001, China;
2. State Key Laboratory of Metastable Materials Science and Technology, Yanshan University, Qinhuangdao 066004, China

Received 10 May 2011; accepted 25 July 2011

Abstract: The influence of cooling rate on the microstructure and nanohardness of the rapidly solidified Ti−48%Al alloys prepared by melt spinning method was studied. The results show that the microstructure of the rapidly solidified ribbons is refined and homogenized compared with that of the conventionally cast mother alloy. With increasing the cooling rate, the grain size decreases greatly. The relationship between the ribbon thickness and the wheel speed was examined, and the effect of the wheel speed on the cooling rate was also studied. It was found that the ribbon thickness decreases inversely with the wheel speed. The nanohardness increases with increasing cooling rate due to the grain size strength.

Key words: rapid solidification; microstructure; cooling rate; TiAl intermetallics

1 Introduction

TiAl intermetallics as a potential high temperature structural material have attracted attention due to their low density, high oxidation resistance and high-temperature strength, etc [1−3]. However, since the ductility of these alloys is rather poor, its applications are restricted [4]. This property has been the subject of intense investigation recently, and it is related to the crystal structure of TiAl which exhibits $L1_0$ face centered tetragonal structure consisting of alternating (002) planes of Ti and Al [5−7].

Rapid solidification technique is a method to solve this problem by refining and homogenizing the microstructure [8−9]. Compared with the conventional solidification techniques, rapid solidification technique increases the solubility of alloying elements and impurities, produces microstructures with refined grain sizes and reduces levels of segregation. Furthermore, it is possible to produce quasicrystals, nanocrystalline and amorphous alloys when cooling metallic melts at cooling rates exceeding 10^4 K/s by rapid solidification technique [10]. Rapid solidification process is therefore used increasingly to manufacture metallurgical materials which take the advantage of these improved properties in various applications [11−12]. The microstructure of rapidly solidified alloys bears strong relationship with the cooling rate. Desired structure can be obtained by controlling the cooling rate. In melt spinning method, there are many processing parameters influencing cooling rate, such as wheel speed, melt temperature, gas ejection pressure, among which the wheel speed is the easiest to control [13−15]. The cooling rate increases linearly with the wheel speed [16]. Therefore, the wheel speed is selected for analyzing the effect of cooling rate on the microstructure of TiAl alloys.

In the present study, binary Ti−48Al alloy was rapidly solidified into the form of ribbon using melt spinning at the wheel speed varying from 10 to 30 m/s. The evolution of the microstructures and nanohardness was studied using XRD, SEM and Nanoindentor XP tester.

2 Experimental

A TiAl alloy with 48% Al (molar fraction) was produced from sponge titanium (99.95%) and aluminum ingot (99.99%) under purified argon. The charges of 3 kg were melted in an induction furnace with a water cooled copper crucible under purified argon. The molten metal was poured into a graphite mould under gravity. The

Foundation item: Project (200806) supported by the State Key Laboratory of Metastable Materials Science and Technology, China
Corresponding author: ZHU Dong-dong; Tel: +86-451-86403150; E-mail: zhudd8@163.com

samples for rapid solidification were cut into cylinders with size of d 8 mm×10 mm by electrical discharge machine. The rapidly solidified ribbons were produced under a low pressure atmosphere of argon by chill block melt spinning onto a copper roll. The alloy charge was heated up to 50−100 K above the corresponding liquidus temperature by high frequency induction heating. After that, the molten alloy was jetted to force the metal through a diameter of 1 mm orifice at the bottom of the crucible onto the inner periphery of a pure copper wheel. The speed of the copper wheel was varied between 10 to 30 m/s and the argon pressure was about 0.04 MPa.

After rapid solidification, the phase constitution was characterized by D/max−RB X-ray diffractometer with monochromatic Cu K_α radiation. SEM observations were carried out on polished sample surfaces after etching with Kroll's reagent (5% HNO_3+5% HF+90% H_2O, volume fraction), using HITACHI S−4700. The chemical composition of the phases was detected by energy dispersive spectroscopy (EDS) affiliated to SEM. The thicknesses of the melt spun ribbons were initially measured with a micrometer. Nanohardness measurements of the polished specimens were carried out on a Nanoindentor XP tester equipped with continous stiffness measurement (CSM).

3 Results and discussion

3.1 Effect of cooling rate on phase composition of Ti−48Al alloy

Figure 1 shows the XRD patterns of conventionally cast alloys and the rapidly solidified samples. From Fig. 1(a), it can be seen that the sample is composed of α_2-Ti_3Al phase and γ-TiAl phase. For the rapidly solidified alloy, the intensity of the α_2 phase peaks increases with the increase in the cooling rate, which means that the volume fraction of the α_2-Ti_3Al phase

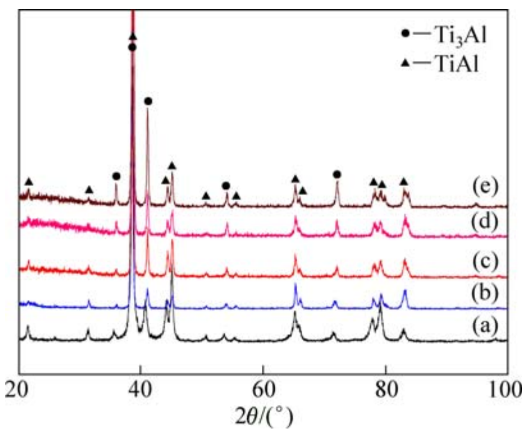

Fig. 1 XRD patterns of Ti−48Al alloy solidified at various wheel speeds: (a) Conventionally cast alloy; (b) 10 m/s; (c) 15 m/s; (d) 20 m/s; (e) 30 m/s

increases with the wheel speed increasing. The intensity of the γ phase peaks decreases with the cooling rate, indicating the increased wheel speed leads to the volume fraction of γ phase decrease. The peaks of the α_2 phase shift to higher angles, indicating that the lattice parameter decreases with cooling rate caused by the distortion of crystal lattice.

3.2 Effect of cooling rate on thickness of rapidly solidified TiAl ribbons

Table 1 shows the average ribbon thicknesses and widths at each wheel speed for rapidly solidified Ti−48Al ribbons. In this study, the variation of wheel speed from 10 to 30 m/s results in a gradual decrease in thickness and width, as seen from Table 1. Similar results were also obtained by other investigators [14].

Table 1 Average ribbon thickness and width calculated at various wheel speeds

Wheel speed/ ($m\cdot s^{-1}$)	Ribbon width/ mm	Ribbon thickness/ μm
10	4.46	137
15	3.77	92
20	2.83	70
30	1.70	42

GILLEN and CANTOR [16] observed that the ribbon emerged from a puddle of a few millimeters width and height with high speed camera [13]. But the formation of the ribbon was very complex. The melt was dragged out by the argon and then solidified in a extremely short time. The variation of ribbon thicknesses and widths is related to the distance which is moved by the melt until it solidifies. When the gas ejection pressure is stable, the quantity of the melt dragged out by the gas is constant. At higher speed, the length moved by the melt is higher. It can be understood in terms of more rapid removal of liquid from the melt, which leads to the decrease of the ribbon thicknesses and widths.

The ribbon thickness can be measured in quantity and used to indicate the cooling rate. GILLEN and CANTOR [16] proved that the cooling conditions during melt-spinning can be considered a near Newtonian, and can describe the relationship between the ribbon thickness and cooling rate during melt-spinning. For wheel speed of Ti−48Al in the range from 10 to 30 m/s, the Nusselt numbers and the heat transfer velocity of the melt decrease with the increase of wheel speeds. Under this condition, the cooling rates are 3.38×10^5, 5.16×10^5, 6.67×10^5 and 1.13×10^6 K/s at wheel speed of 10, 15, 20 and 30 m/s, respectively.

3.3 Microstructure change during rapid solidification

In order to understand the microstructure evolution of Ti−48Al alloy during rapid solidification, the samples were examined by SEM. Figure 2 shows the microstructure of Ti−48Al alloy solidified under different wheel speeds. Figure 3 shows the SEM images of the rapidly solidified microstructure with high magnification. Figure 2(a) illustrates that the as-cast alloy exhibits dendrite structure. The interdendritic segregate phase is γ (γ_s) and the dendritic microstructure is mixture lamellar grains with two phases $\alpha_2+\gamma$.

Figure 2(b) shows the microstructure of rapidly solidified Ti−48Al alloy at a wheel speed of 10 m/s. As can be seen, the microstructure of this ribbon is composed of two phase $\gamma+\alpha_2$. The dominant phase γ can exist both as laths in the transformed lamellae and massive morphology. EDS analysis shows that the Al content in the γ phase and grain boundary is 51.95% and 52.16%, respectively, indicating rapid solidification has homogenized the alloys significantly. With increasing the wheel speed to 15−30 m/s (Figs. 2(c)−(e)), the volume fraction of α_2 phase increases, which is believed to result from solidification. Comparing to the alloy produced at lower wheel speed, the grain size of γ phases decreases dramatically when solidified at higher wheel speed. This is because the increased cooling rates lead to large undercooling and reduced solidification time prior to solidification. As can be seen from Fig. 3, the lamellar structure also decreases with increasing wheel speeds, which can hardly be seen at wheel speed of 30 m/s. This is because the lamellar structure is formed by the terrace-ledge-kink mechanism. In this mechanism, the thickening velocity increases with diffusion coefficient. At the wheel speed of 30 m/s, the diffusion coefficient decreases greatly. So the lamellar structure can hardly be seen.

3.4 Effect of cooling rate on nanohardness of rapidly solidified TiAl ribbons

In this study, the mechanical properties of the samples solidified under different cooling rates are determined by nanohardness measurement. In a typical instrumented nanoindentation test, the applied normal load and depth of penetration are recorded during the

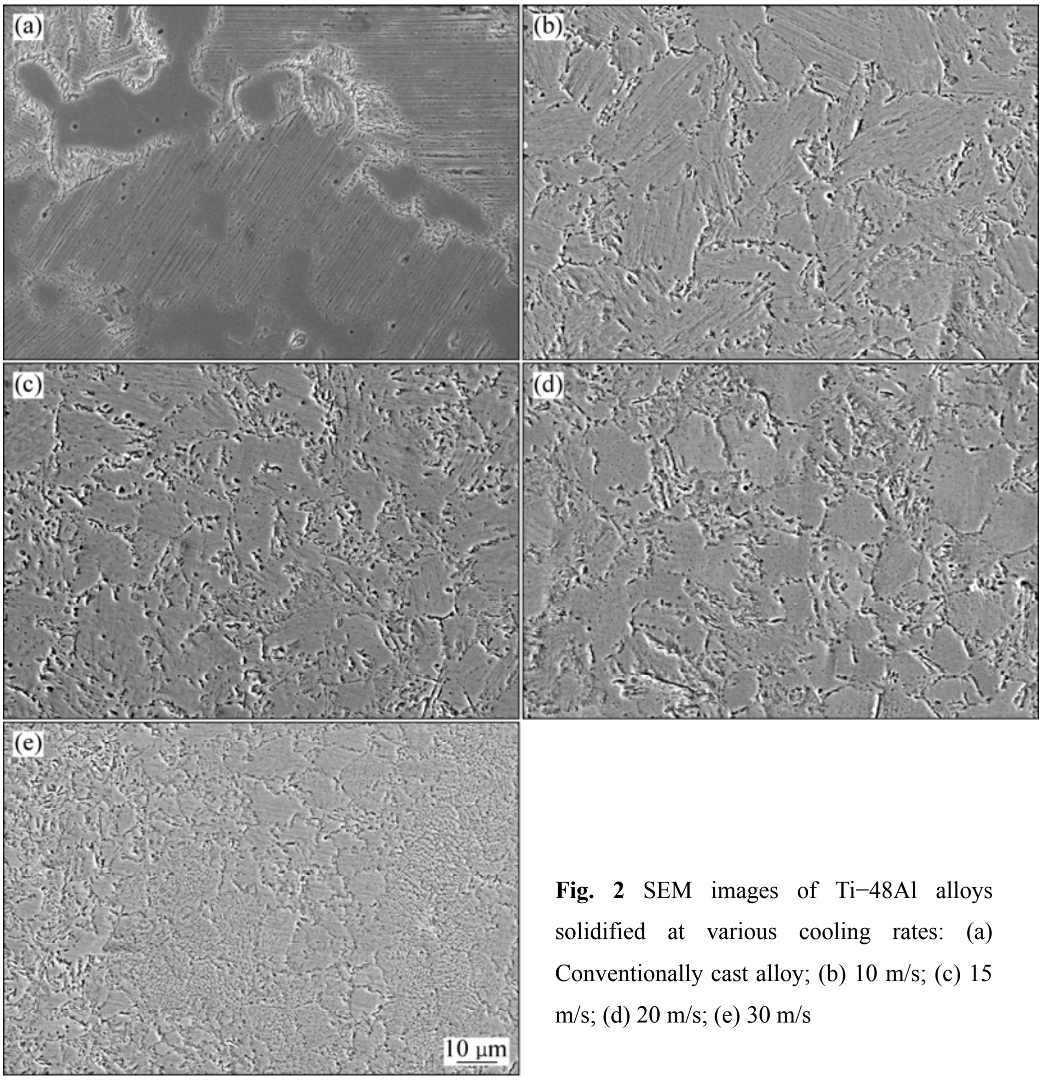

Fig. 2 SEM images of Ti−48Al alloys solidified at various cooling rates: (a) Conventionally cast alloy; (b) 10 m/s; (c) 15 m/s; (d) 20 m/s; (e) 30 m/s

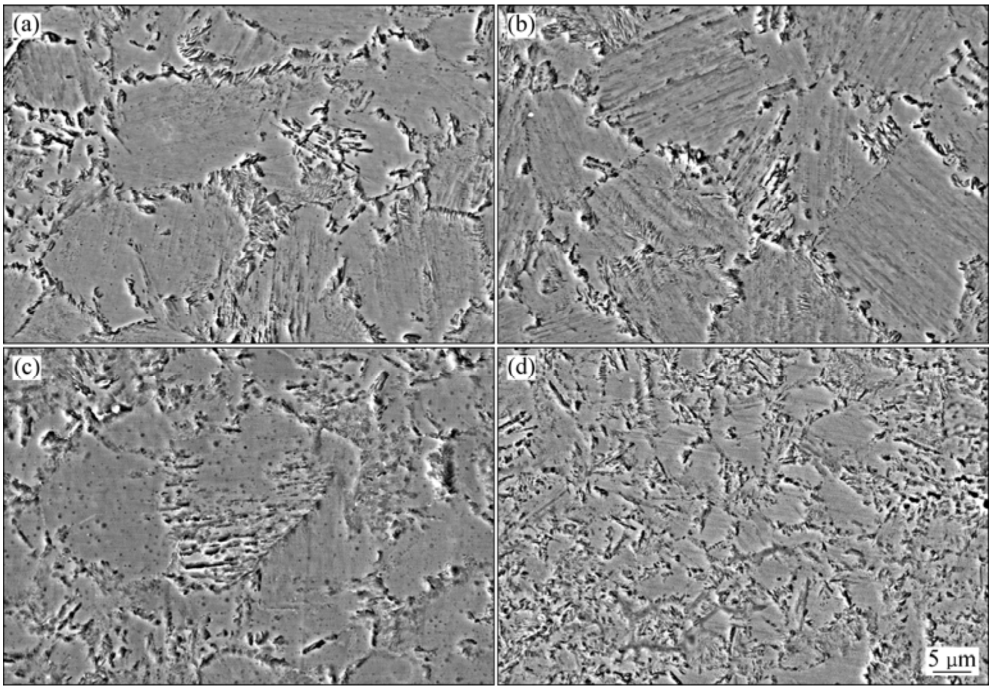

Fig. 3 High magnification SEM images of Ti−48Al ribbons rapidly solidified at wheel speed of 10 m/s (a), 15 m/s (b), 20 m/s (c) and 30 m/s (d)

measurement, while the area of the indent is calculated from the known geometry of the indenter tip. These values can be plotted to result in load—displacement curves.

Figure 4 shows the nanohardness of the rapidly solidified Ti−48Al ribbons at different wheel speeds. It can be seen that the hardness increases with the wheel speed. In solid mechanics, the material hardness is described as the resistance to deformation. According to the analysis in Section 3.3, the grain size of the rapidly solidified ribbon decreases with increasing cooling rate. Hence, the increase of hardness can be attributed to the strength of grain size.

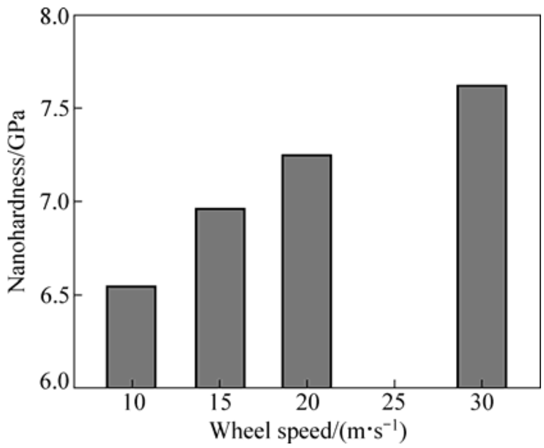

Fig. 4 Nanohardness of rapidly solidified TiAl ribbons at different wheel speeds

4 Conclusions

1) Rapid solidification does not change the phase constitution of Ti−48Al alloy. The ribbon is composed of α_2-Ti_3Al phase and γ-TiAl phase. The volume fraction of α_2 phase increases with increasing cooling rates.

2) With increasing the cooling rate, the thickness and width of the ribbon decrease greatly. The decrease in the ribbon thickness can be understood in terms of more rapid removal of liquid from the melt.

3) The microstructure of Ti−48Al alloy changes greatly under rapid solidification compared with that under normal pressure conditions. The dominant phase is γ which can exist both as laths in the transformed lamellae and massive morphology. The grains size decreases greatly with increasing the cooling rate because of the large undercooling and the reduced solidification time prior to solidification.

4) With increasing the cooling rate, the grain size of the ribbons decreases greatly. Due to the strength of grain size, the hardness increases with the cooling rate.

References

[1] LIU Q, NASH P. The effect of ruthenium addition on the microstructure and mechanical properties of TiAl alloys [J]. Intermetallics, 2011, 19(9): 1282−1290.

[2] LIU Wen-sheng, HUANG Bai-yun, ZHOU Ke-chao, HE Yue-hui, LIU Yong. Lamellae growth in fully lamellar TiAl alloys and its factors [J]. The Chinese Journal of Nonferrous Metals, 2003, 13(1):

153−156. (in Chinese)
[3] RAMANUJAN R V. Phase transformation in γ based titanium aluminides [J]. Int Mater Rev, 2000, 45(6): 217−240.
[4] QU H P, LI P, ZHANG S Q, LI A, WANG H M. The effects of heat treatment on the microstructure and mechanical property of laser melting deposition [gamma]-TiAl intermetallic alloys [J]. Mater Design, 2010, 31(4): 2201−2210.
[5] FU Heng-zhi, GUO Jing-jie, SU Yan-qing, LIU Ling, XU Da-ming, LI Jin-shan. Directional solidification and lamellar orientation control of TiAl intermetallics [J]. The Chinese Journal of Nonferrous Metals, 2003, 13(4): 797−810. (in Chinese)
[6] NOVOSELOVA T, CELOTTO S, MORGAN R, FOX P. Formation of TiAl intermetallics by heat treatment of cold-sprayed precursor deposits [J]. J Alloy Compd, 2007, 436(1−2): 69−77.
[7] IMAYEV R, SALISHCHEV G. Effect of grain size on ductility and anomalous yield strength of micro- and submicrocrystalline TiAl [J]. Scripta Metallurgica et Materialia, 1993, 29(1): 713−718.
[8] YANG W, LIU F, WANG H F, LU B P, YANG G C. Non-equilibrium transformation kinetics and primary grain size distribution in the rapid solidification of Fe–B hypereutectic alloy [J]. J Alloy Compd, 2011, 509(6): 2903−2908.
[9] LAVERNIA E J, SRIVATSAN T S. The rapid solidification processing of materials: science, principles, technology, advances, and applications[J]. J Materials Science, 2010, 45(2): 287−325.
[10] GOGEBAKAN M, UZUN O, KARAASLAN T, KESKIN M. Rapidly solidified Al-6.5 wt.% Ni alloy [J]. Journal of Materials Processing Technology, 2003, 142(1): 87−92.
[11] KARAKOSE E, KESKIN M. Effect of solidification rate on the microstructure and microhardness of a melt-spun Al−8Si−1Sb alloy [J]. J Alloys Compd, 2009, 479(1−2): 230−236.
[12] WANG N, WEI B. Rapid solidification of undercooled Cu-Ge peritectic alloy [J]. Acta Mater, 2000, 48(8): 1931−1938.
[13] CANTOR B, KIM W T, BEWLAY B P, GILLEN A G. Microstructure-cooling rate correlations in melt-spun alloys [J]. J Mater Sci, 1991, 26(5): 1266−1276.
[14] TAHA M A. Geometry of melt-spun ribbons [J]. Mater Sci Eng A, 1991, 134: 1162−1165.
[15] LIU Z G, CHEN Y Y, CHAI L H, KONG F T, DAVIES H A. Production and characterization of TiAl ribbons with Y additions [J]. Transactions of Nonferrous Metals Society of China, 2006, 16: s711−s714
[16] GILLEN A G, CANTOR B. Photocalorimetric cooling rate measurements on a Ni-5wt.% Al alloy rapidly solidified by melt spinning [J]. Acta Metall, 1985, 33(10): 1813−1825.

快速凝固 Ti−48Al 合金的组织及纳米硬度

王宏伟 [1,2]，朱冬冬 [1]，邹鹑鸣 [1]，魏尊杰 [1]

1. 哈尔滨工业大学 材料科学与工程学院，哈尔滨 150001；
2. 燕山大学 亚稳材料制备技术与科学国家重点实验室，秦皇岛 066004

摘　要：研究冷却速度对熔体旋转法制备的快速凝固 Ti−48%Al 合金组织的影响。结果表明：同传统凝固相比，快速凝固明显细化了 Ti−48%Al 合金的组织，并使合金的成分变得均匀。随着冷却速度的增加，合金的晶粒明显细化。研究薄带厚度、辊速与冷却速度的关系。随着辊速的增加，冷却速度增加，薄带厚度呈减小的趋势。由于细晶强化的作用，快速凝固薄带的纳米硬度随着冷却速度的增加而增加。

关键词：快速凝固；组织；冷却速度；钛铝金属间化合物

(Edited by FANG Jing-hua)